OPEN

Potential and Most Relevant Applications of Total Body PET/CT Imaging

Abass Alavi, MD, Babak Saboury, MD, MPH,*† Lorenzo Nardo, MD, PhD,‡ Vincent Zhang, BA,* Meiyun Wang, MD, PhD,§ Hongdi Li, PhD,|| William Y. Raynor, MD,* Thomas J. Werner, MSE,* Poul F. Høilund-Carlsen, MD, DMSci,¶** and Mona-Elisabeth Revheim, MD, PhD, MHA*††‡‡*

Abstract: The introduction of total body (TB) PET/CT instruments over the past 2 years has initiated a new and exciting era in medical imaging. These instruments have substantially higher sensitivity (up to 68 times) than conventional modalities and therefore allow imaging the entire body over a short period. However, we need to further refine the imaging protocols of this instrument for different indications. Total body PET will allow accurate assessment of the extent of disease, particularly, including the entire axial and appendicular skeleton. Furthermore, delayed imaging with this instrument may enhance the sensitivity of PET for some types of cancer. Also, this modality may improve the detection of venous thrombosis, a common complication of cancer and chemotherapy, in the extremities and help prevent pulmonary embolism. Total body PET allows assessment of atherosclerotic plaques throughout the body as a systematic disease. Similarly, patients with widespread musculoskeletal disorders including both oncologic and nononcologic entities, such as degenerative joint disease, rheumatoid arthritis, and osteoporosis, may benefit from the use of TB-PET. Finally, quantitative global disease assessment provided by this approach will be superior to conventional measurements, which do not reflect overall disease activity. In conclusion, TB-PET imaging may have a revolutionary impact on day-to-day practice of medicine and may become the leading imaging modality in the future.

Key Words: FDG, global disease assessment, musculoskeletal disease, NaF, total body PET, vascular disease

(*Clin Nucl Med* 2022;47: 43–55)

Received for publication August 12, 2021; revision accepted September 13, 2021.

From the *Department of Radiology, Hospital of the University of Pennsylvania, Philadelphia, PA; †Department of Radiology and Imaging Sciences, National Institutes of Health, Clinical Center, Bethesda, MD; ‡Department of Radiology, University of California, Davis, Sacramento, CA; §Department of Radiology, Henan Provincial People's Hospital, Henan, China; ||United Imaging Healthcare, Houston, TX; ¶Department of Nuclear Medicine, Odense University Hospital; **Research Unit of Clinical Physiology and Nuclear Medicine, Department of Clinical Research, University of Southern Denmark, Odense, Denmark; ††Division of Radiology and Nuclear Medicine, Oslo University Hospital; and ‡‡Institute of Clinical Medicine, Faculty of Medicine, University of Oslo, Oslo, Norway.

Conflicts of interest and sources of funding: L.N. is the principal investigator of a service agreement with United Imaging Healthcare. L.N.'s employer (University of California, Davis) has a revenue-sharing agreement with United Imaging Healthcare. A.A. is a consultant to United Imaging Healthcare. The remaining authors declare no conflicts of interest.

This article does not contain any studies with human participants or animals performed by any of the authors. Images were collected from existing published literature.

Correspondence to: Mona-Elisabeth Revheim, MD, PhD, MHA, Rikshospitalet, Postbox 4950 Nydalen, 0424 Oslo, Norway. E-mail: mona.elisabeth.revheim@ous-hf.no; m.e.rootwelt-revheim@medisin.uio.no.

ISSN: 0363-9762/22/4701–0043
DOI: 10.1097/RLU.0000000000003962

The invention of x-ray by Roentgen opened up a new era in medicine and revolutionized its practice substantially over time. Planar imaging by conventional x-ray was suboptimal for detection and cauterization of many diseases and disorders and therefore was somewhat limited in its domain of applications. The introduction of x-ray CT in the early 1970s by Hounsfield[1] changed the success of medical imaging in the day-to-day practice and research in medicine. In its early years, imaging with CT was very limited and cumbersome in scope, but its capabilities have substantially improved over the ensuing decades. As such, currently x-ray–CT is the medical imaging modality of choice for assessing numerous diseases and disorders. A decade after the introduction of CT, MRI was developed by Lauterbur[2] and Mansfield and Maudsley,[3] and this further enhanced the role and the importance of medical imaging in medicine. The impact of MRI was particularly impressive in assessing and managing diseases that affect soft tissue organs such as the brain, musculoskeletal (MSK) structures, and cardiovascular system. While tomographic imaging was originally used by investigators at the University of Pennsylvania in the 1960s with conventional single gamma emitting radiotracers,[4] the impact of this approach was not completely realized until a decade or two later when scintillation camera-based tomographic instruments were designed and introduced to the day-to-day practice of medical imaging.[5,6] This tomographic instrument, single-photon emission CT is the workforce of modern practice of the specialty of nuclear medicine. However, over the past decade, despite constant efforts made to synthesize biologically important single-photon–emitting compounds to assess the disease process at the molecular and cellular level, the yield has been very limited and somewhat disappointing.[7] Therefore, over the past 4 to 5 decades, major attempts have been made to synthesize powerful radiotracers by labeling positron-emitting radioactive elements to biologically active compounds. However, the annihilation of positrons results in emission of high-energy gamma rays, which require especially designed instruments for their successful applications in medical research and practice of medicine. Attempts to design and build successful PET instruments were initiated by investigators at the Washington University in the early 1970s, and by the late 1970s and early 1980s, such instruments became a reality, which brought about and initiated a new era in the specialty of molecular imaging.[8] The introduction of ^{18}F-fluorodeoxyglucose (FDG) as a powerful PET tracer by investigators at the University of Pennsylvania and Brookhaven National Laboratory combined with the well-designed PET instrumentation further advanced the role and potential impact of this modality in medicine and biological research.[9,10]

By now, it is well established that structural imaging alone has certain limitations. Structural techniques are insensitive for detecting disease activity at diagnosis and following its course over time. In particular, structure-based methodologies are insensitive to detecting early response to treatment. Therefore, findings from such imaging studies have led to initiating potent therapeutic interventions

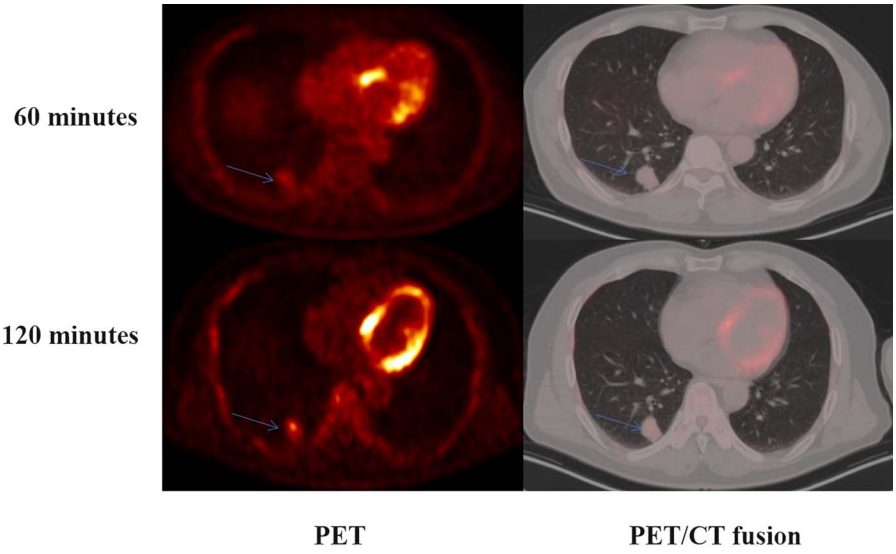

FIGURE 1. A 62-year-old man coughing for 1 week. Total body FDG PET/CT showed the right lower lobe nodule measuring 1.7 × 2.2 cm (arrow). Delayed imaging showed a progressive increase in metabolism (SUVmax 3.4 vs 6.2). The nodule was pathologically proven to be adenocarcinoma.

that have had no or limited benefits to the patient but with significant adverse effects and have been life threatening at times. Similar to pathology that evolved from anatomical-pathology to histopathology and molecular/immunohistochemical characterization, the trajectory of medical imaging growth is indeed toward molecular and functional imaging. As such, combining the results provided by the molecular imaging techniques such as PET with those of the structural modalities such as CT or MRI has brought about a major change to the daily practice of the specialty of radiology and nuclear medicine. In 2001, investigators at the University of Pittsburgh were the first to combine the CT and PET instruments as a single hybrid unit that has allowed assessing disease activity at the structural and functional level sequentially in the same sitting.[11]

Because of technical limitations, the initial PET instruments were designed with a very small field of view, which allowed imaging of only a fraction of the body structures at one time. This necessitated imaging of the intended organs and anatomic sites for an extended period, which limited its clinical use. Over the years, the field of view of modern PET instruments increased from a few centimeters up to 20 to 25 cm. Despite these improvements, even with modern PET instruments, screening a large segment of the body for diseases that are systemic and widespread in nature requires imaging for an extended period.

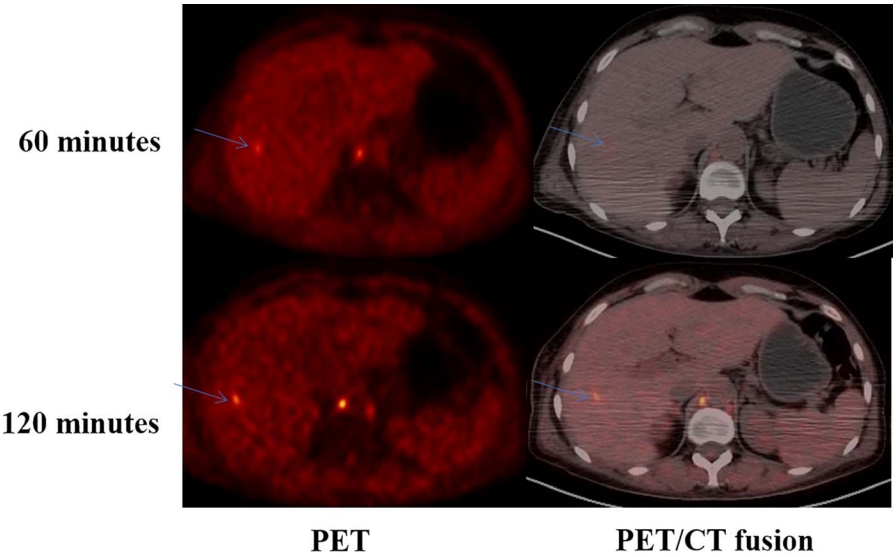

FIGURE 2. FDG PET/CT in a 48-year-old woman with nasopharyngeal carcinoma after radiotherapy and chemotherapy. A new nodular low-density shadow with a diameter of approximately 0.7 cm appeared in the liver, and the metabolism of delayed imaging continued to increase (SUVmax 3.0 vs 4.0). Liver metastases were diagnosed by clinical follow-up.

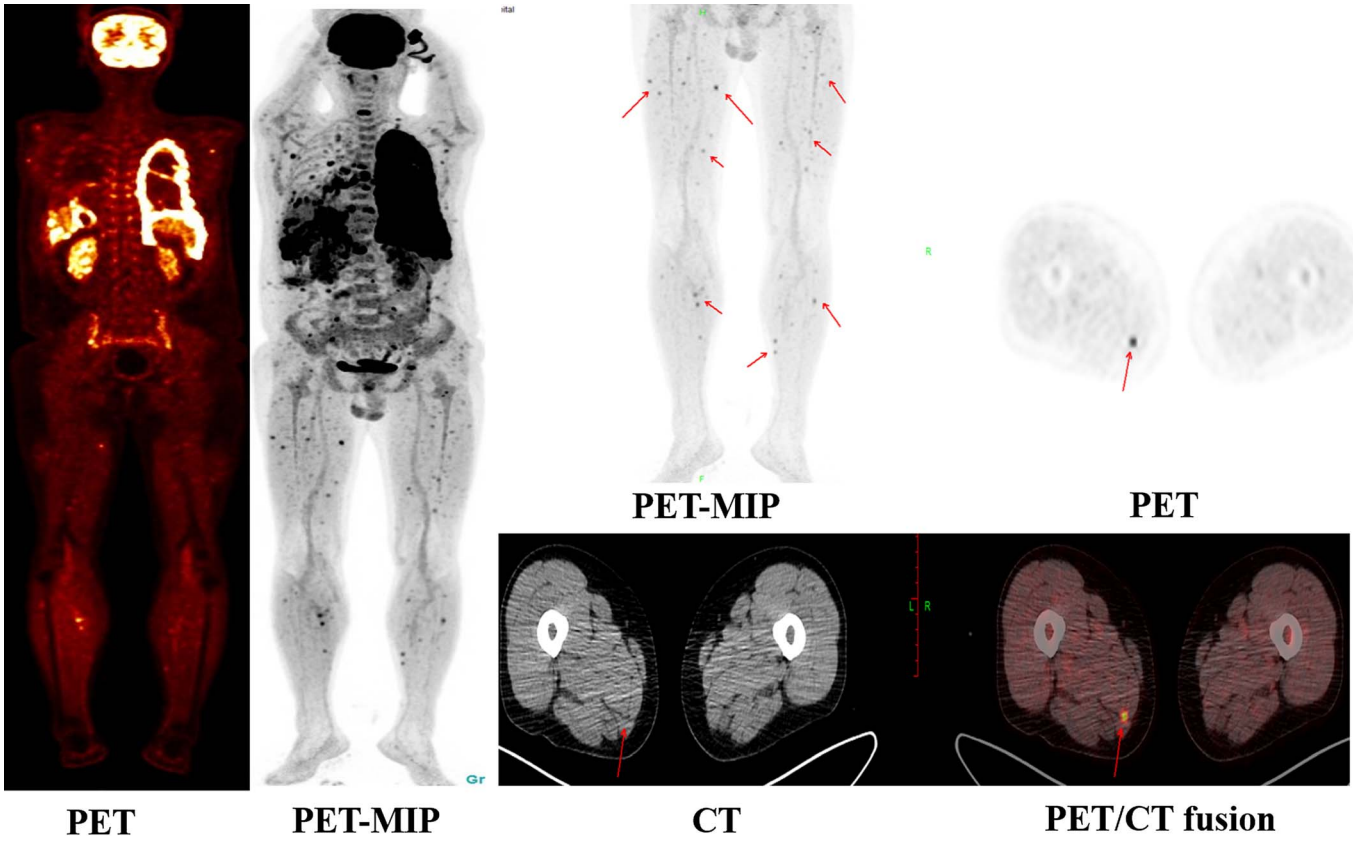

FIGURE 3. One month after operation, there were multiple metastases in both lungs, pleura, spleen, peritoneum, greater omentum, skeletal system, and muscles of the whole body in a 46-year-old man with liver cancer. Total body FDG PET/CT showed multiple nodules with high metabolism in the distal muscles of the extremities.

During the past several years, investigators at the University of California, Davis, have further enhanced the performance of PET by increasing its ability to screen the entire body with a single data acquisition, using low radiotracer dose or shorter acquisition time, or delayed imaging and/or combining this parameters.[12] The revolutionary impact of total body PET (TB-PET) imaging may be far reaching and may substantially change the role of imaging in medicine. This PET instrument is combined with a CT machine, and therefore, functional and structural images can be assessed side by side or superimposed.

In this editorial, we describe several domains where we believe TB-PET/CT imaging may have the highest impact in the future.

MALIGNANT DISORDERS

Since its introduction in the 1970s, FDG PET has been extensively tested and validated as a powerful imaging modality for the diagnosis and management of numerous malignant disorders.[9,13] As such, FDG-PET has played a major role in clinical routine of medical, surgical, and radiation oncology and is considered as an essential modality for optimal management of patients with cancer. PET has allowed early and accurate diagnosis of cancer, staging its extent, detecting response to treatment, and assessing patients for recurrence at later times during the course of the disease.[14] Conventionally, FDG PET images are acquired approximately 1 hour following the administration of this radiotracer. Based on experience that has been gained by several groups including that of our own, it has become clear that FDG uptake increases over time and reaches a plateau at 4 to 5 hours,[15–17] and several types of tumor (eg, gliomas) have peak of uptake significantly later than the conventional 1-hour uptake time used on conventional imaging. Furthermore, radiotracer activity in the blood and background tissues decreases over time, and the combination of these 2 changes leads to a higher contrast between the tumor metabolic activity and the surrounding background (Figs. 1–2).[18] As a result, the sensitivity of this modality as a biomarker for disease activity in cancer improves significantly by this approach. The standard protocol of performing FDG PET 1 hour after administration of the compound results in overlooking disease sites at the primary and metastatic sites. This practice has been dictated by the low sensitivity of conventional PET instruments that allow detecting only a fraction of the emitted gammas from the patient being imaged. By now, it is well established that the sensitivity of TB-PET instruments is approximately 15 to 68 times higher than that of conventional PET/CT machines in the market (Fig. 3).[19–21] The high sensitivity of this instrument allows decreasing the dose of the administered radioactive compounds and reduces the radiation exposure to the patient, especially important for children and young adults. Overall, the high efficiency of the simultaneous TB-PET/CT imaging techniques will allow imaging for up to 12 hours (6–7 ^{18}F half-lives) after the administration of FDG. Different types of malignant cells accumulate variable amounts of FDG, probably due to varying amounts of glucose-6-phosphatase concentration. More aggressive proliferating cancer cells tend to have lower levels of glucose-6-phosphatase and exhibit rising levels of FDG uptake over time, whereas the opposite is applicable in less aggressive or proliferative cancer cells and inflammatory cells.[16,22–24]

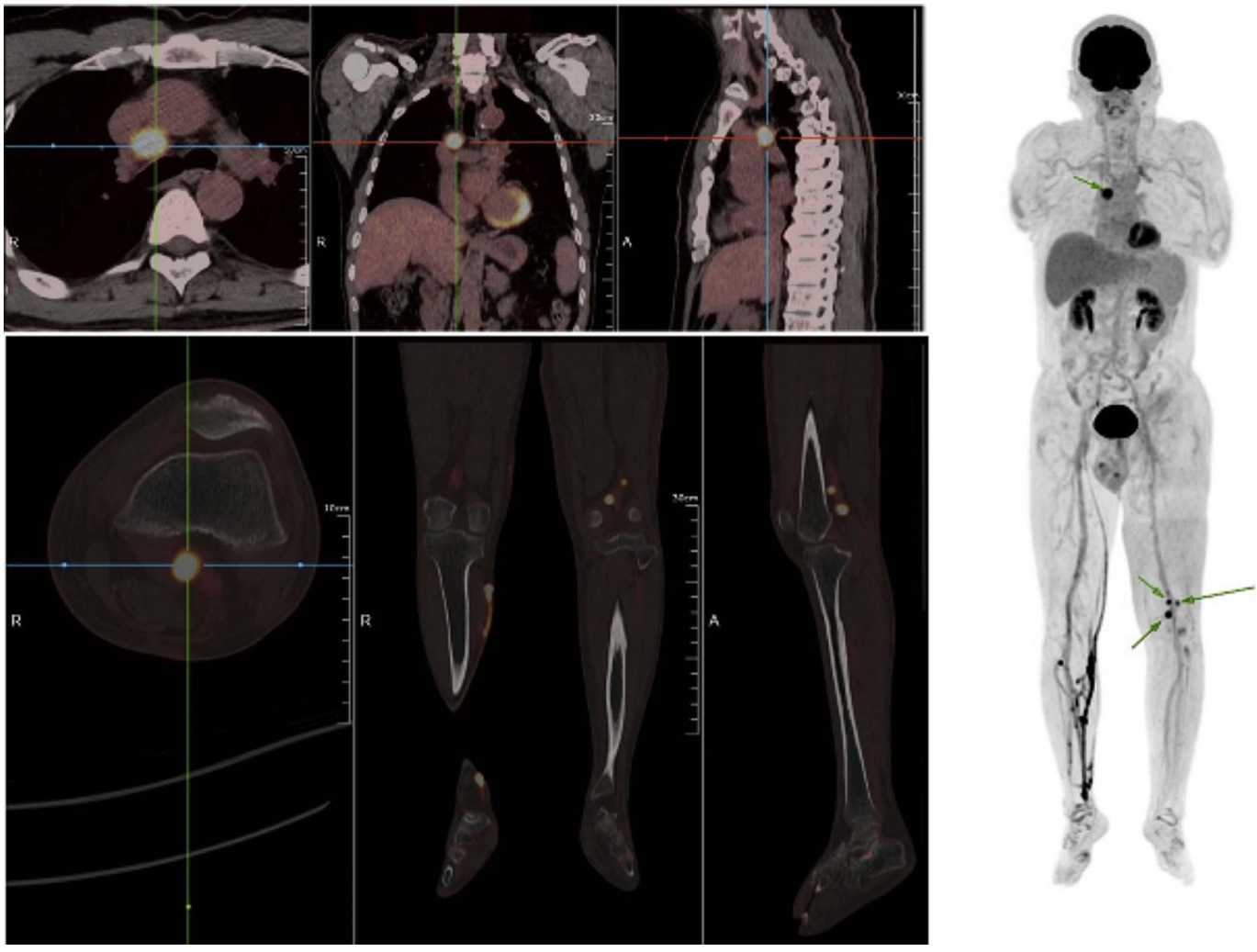

FIGURE 4. Left feet melanoma with lymph nodal metastases in left popliteal fossa and mediastinum. A 60-year-old man with history of melanoma. Status post left thumb and second toe resection, popliteal fossa lymph node dissection performed 8 months ago. FDG PET/CT imaging (dose 3.7 MBq/kg, acquisition time 5 minutes) demonstrated an FDG-avid lymph node in mediastinum and a group of FDG-avid lymph nodes in left popliteal fossa. Ultrasound-guided bronchoscopy biopsy of the mediastinal lymph showed metastatic melanoma. Reproduced with permission from Sui et al.[25]

This substantially enhances the ability to detect cancer at different locations in the body (Fig. 4).[25] The ability to acquire delayed images may have a major impact for optimal management of patients with several malignancies. In particular, the impact will be significant when the exact location and the extent of the disease are of great importance for effective management by surgical interventions and radiation therapy (Figs. 5).[26] Moreover, several cancers are characterized by a biological heterogeneity, and there may be large variations within as well as between tumors and metastases within the same patient. Inevitably, classification and prognostication based on one or a limited number of biopsies are prone to sampling errors as the biopsies may not be representative for the disease heterogeneity. The response to treatment may also differ, and TB imaging may provide a full overview. Overall, TB-PET imaging may be of great importance in improving diagnosis and overall management of oncologic patients.

Vascular disorders and complications are commonly observed in patients with malignancies, and some may prove to be fatal in this population.[27–29] In particular, the incidence of deep venous thrombosis (DVT) is relatively common in patients with cancer.[30] In fact, the second most common cause of mortality in this population is due to pulmonary embolism (PE), which is potentially fatal. FDG has been shown to be taken up by the activated cells in the clots in the venous system. Uptake of FDG has been shown in the actively forming clots by in vitro techniques, in animals and in human studies.[31–33] There is clear evidence that FDG PET/CT imaging approach may prove to be of great importance in detecting clots in the venous system and prevent serious consequences of this common human disease. This PET imaging approach may revolutionize the management of unknown DVT in patients with and without cancer and improve the outcome in this population (Figs. 6 and 7).[34,35] Because patients with cancer are frequently examined by FDG PET for the routine management of their underlying disease, it is predicted that the TB-PET imaging approach will allow detection of clots in various locations throughout the body. Currently, the existing protocols suggest imaging the body from the base of the skull to the upper-mid thigh region. This procedure is adopted by two well-known facts: malignant cells metastasize mostly to the

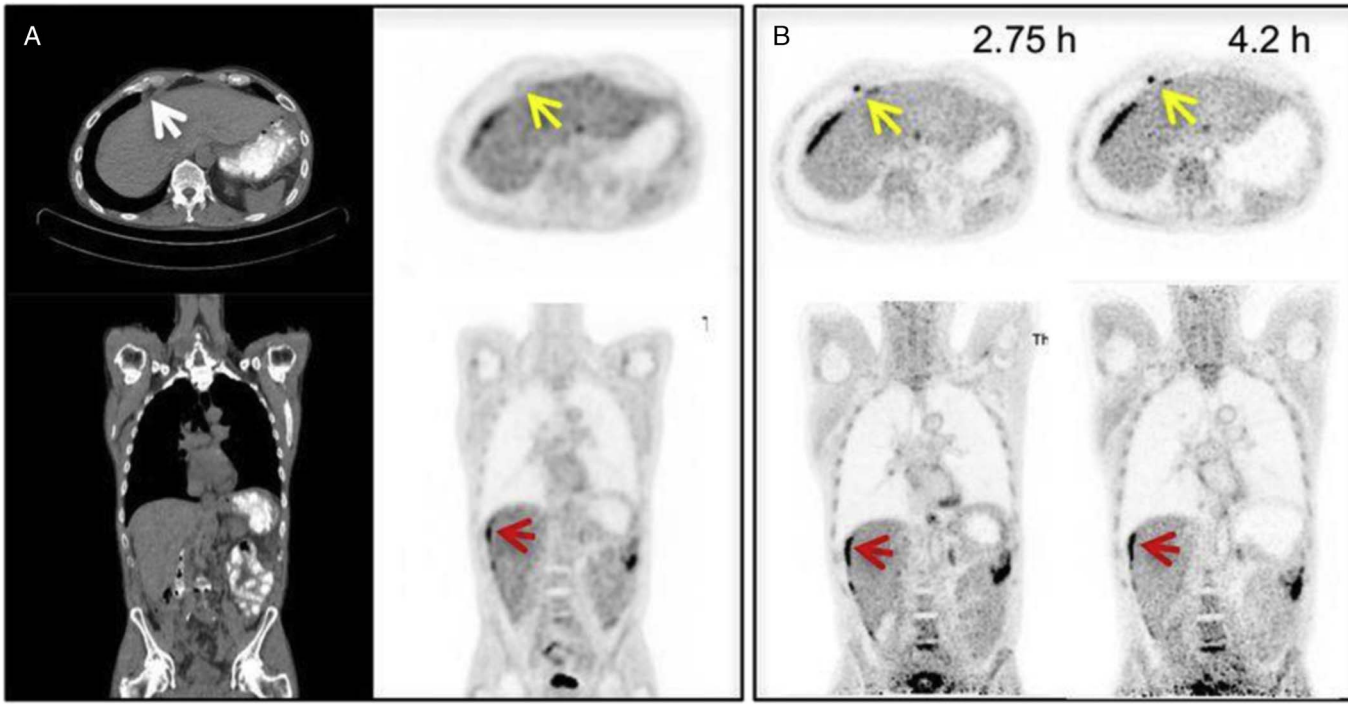

FIGURE 5. **A**, Standard-of-care FDG PET/CT images (transverse and coronal) from a patient with metastatic colon cancer. **B**, PennPET image acquired 2.75 and 4.2 hours after injection (10-minute scans) demonstrated better delineation of perihepatic disease (red arrow) compared with standard-of-care PET. An epiphrenic lymph node (yellow arrow) is also only seen on the delayed PennPET images. Reproduced with permission from Nardo and Pantel.[26]

red marrow, which is prevalently located in the axial skeleton and proximal appendicular skeleton. Therefore, if the aim of FDG PET imaging is to detect metastasis to the skeletal system, the current imaging protocol is logical and allows detection of the disease at these predisposed sites in the bony structures, overlooking sites where the presence of bone metastasis is unlikely. Also, imaging the entire lower extremities will almost double the amount of time to complete the scan, increasing number of bed positions and often repositioning the patients in the scanner. Unfortunately, this approach overlooks the presence of clots in the lower thighs and the calves, which are common locations for venous thrombosis. The data that have accumulated over the years have shown the efficacy of FDG PET in detecting and assessing the extent of clots in the venous system throughout the body. We also believe delayed TB imaging with FDG PET will result in higher sensitivity of this technique for clot detection in the entire body. In other words, enhanced FDG uptake in the clots and significantly deceased blood pool activity in the venous system over time may improve the detection of the clots in the venous system.

In recent years, numerous research and clinical observations have demonstrated that patients with cancer are also prone to developing atherosclerosis (AS) in the arterial system throughout the body.[36–38] It is well established that patients with various malignancies are subject to developing AS, which includes suffering from high incidence of heart attacks and strokes compared with the control population.[39,40] The data with both FDG and ^{18}F-labeled sodium fluoride (NaF) have shown that these two PET tracers can successfully detect atherosclerotic plaques throughout the body.[27,41–43] While FDG PET imaging allows visualizing inflammatory lesions, NaF detects molecular calcification in the plaques. Therefore, by performing delayed TB imaging, it will be feasible to better characterize AS throughout the body and initiate appropriate therapeutic interventions to prevent complications from this potentially fatal disease.[44] In particular, delayed imaging is going to be essential for detection and quantification of atherosclerotic plaques in the affected arteries.

ATHEROSCLEROSIS

Atherosclerosis is the main cause of cardiovascular diseases (CVDs), which are the number one cause of death globally. In 2016, 17.9 million people died of CVDs, representing 31% of all global deaths, and of these, 85% were due to heart attack and stroke.[45,46] Despite a decline in the death rate from CVDs, they remain the leading cause of death in the United States, responsible for 840,768 deaths (635,260 cardiac) in 2016,[47] and continue to be a major cause of the morbidity and mortality among the elderly population worldwide. Clinical assessment and some diagnostic procedures such as contrast-enhanced angiography are of limited value for detecting the atherosclerotic plaques and monitoring response to therapeutic interventions.[48] The introduction of x-ray–CT in the 1970s allowed detection and characterization of the calcified plaques in the coronary and major arteries in the advanced stages of the disease.[49] However, this finding on CT scans is of limited value in effective management of patients with the disease. This is mainly due to the fact that calcification visualized by CT represents an advanced stage of the atherosclerotic process, which is irreversible with current treatments. In recent years, with advances that have been made in CT imaging instruments, it is feasible to perform noninvasive angiography of the coronary arteries and generate high-quality scans with great structural detail.[50] However, by now, it is well-established that structural abnormalities, such as narrowing of the arterial lumen by the atherosclerotic disease including gross calcification, are of limited value in predicting plaque rupture and therefore thrombosis in the

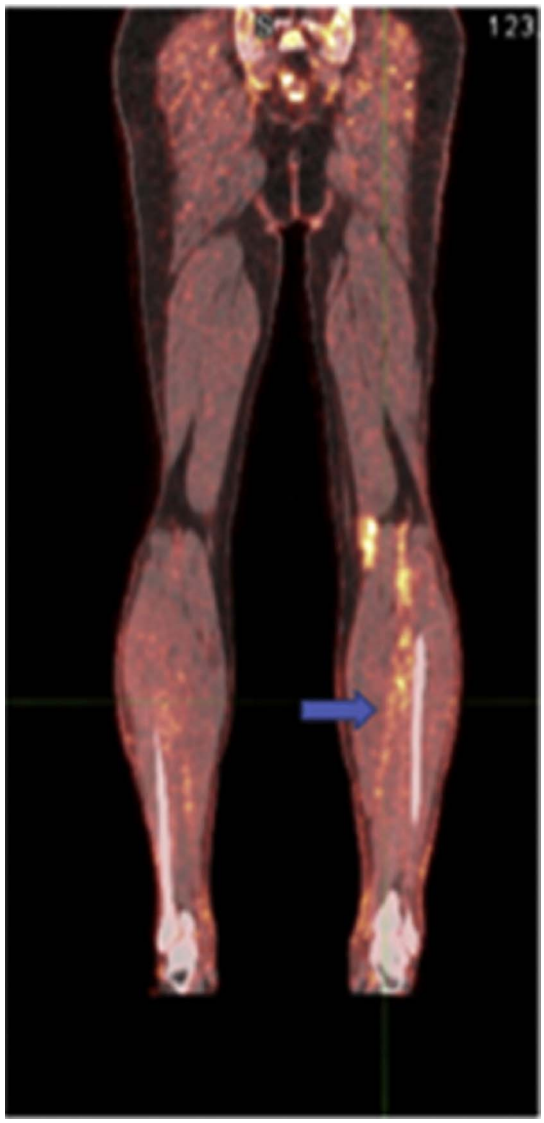

FIGURE 6. A 65-year-old man with melanoma on the left upper back, on BRAF/MEK inhibitor, which was held, secondary to toxicity, with biopsy-proven gastric metastasis and left axillary nodal metastasis. One day before the PET scan, the patient had 2+ edema from the mid-upper arm to the hand and 1+ edema in the left calf and foot. A coronal fused FDG PET/CT image shows increased metabolic activity within the left lower leg veins (arrow) corresponding with an acute deep vein thrombosis. Reproduced with permission from Saboury et al.[34]

vessels.[42,51,52] Thus, there is a dire need for powerful technologies that can assess overall atherosclerotic burden in the early stages of the disease and therefore prevent irreversible complications that are associated with the process.[53,54]

As such, FDG PET imaging has been used for the detection of atherosclerotic plaque because they contain a large number of macrophages in the active stages of this disease.[55,56] In contrast, imaging with NaF allows visualizing calcification at the molecular level in the plaques.[56] Recent data from our group have shown greater sensitivity for visualizing calcification with NaF compared with FDG for detecting inflammation in the atherosclerotic plaques and a more consistent association between arterial NaF uptake than FDG uptake and CV risk factors.[55] Therefore, based on the data that are available, it is likely that NaF PET imaging may become the technique of choice to detect and monitor the course of AS in the future, although this remains to be clearly demonstrated in longitudinal follow-up studies. Furthermore, it has become apparent that global disease assessment with the established PET techniques is superior to measurements at the regional level for the quantification AS burden in the coronary and major arteries.[41,57]

Based on dynamic imaging with NaF and FDG, it has been shown that with prolonged uptake time and delayed image acquisition, PET images reveal higher contrast between atherosclerotic plaques and the surrounding structure (Figs. 8-10).[25,42,58,59] This phenomenon is mainly due to significant clearance of both agents from the circulation and the surrounding tissue structures, which leads to a higher contrast between the plaques and the background activity. However, there are some limitations to using current PET instruments for delayed imaging. Although this method improves target-to-background contrast, using the standard PET machines results in generating images with suboptimal number of counts and therefore greater amount of noise in reconstructed scans. High sensitivity of TB-PET instruments would allow imaging ^{18}F-labeled tracers up to several hours and generate scans with the same noise characteristics as those of current PET instruments at 1 hour.[44] Recent studies suggest that the ideal image acquisition time for detecting AS plaques with NaF and FDG would be in the range of 3 to 4 hours after the administration of these compounds.[60] Delayed whole-body images with uptake times extended from 1 hour (current) to 3 hours (delayed) would only represent an approximate one-half decrease (53%) in tracer activity, and therefore imaging protocols with a TB-PET scanner could allow for significant reductions in either dose or scan time (or a combination of both), as well as delayed acquisition (Fig. 11).[61] Decreasing the administered dose and delaying imaging would allow performing multiple scans in the same patient with AS over time to assess the efficacy of various interventions while still keeping the total accumulated radiation dose to the patient to a minimum according to ALARA (as low as reasonably achievable) principles. In contrast to many chronic and disabling diseases, there exist some very effective drugs such as statins for treating AS.[62,63] Because the mechanisms of action of these drugs vary substantially among them, efforts should be made to test and personalize the best treatment option for an individual patient. The high performance of TB-PET may be ideally suited for the diagnosis and management of patients with AS.

BONE METABOLISM AND OSTEOPOROSIS

Metabolic bone disorders are one of the leading causes of morbidity and mortality in both chronic diseases (such as cancer and autoimmune diseases) and normal aging population. Osteoporosis is a common metabolic bone disease that affects a large segment of the world's population. This disease is particularly common in older subjects with a substantially high incidence in postmenopausal women.[64,65] Osteoporosis is associated with significant morbidity and is a common cause of fractures in the elderly population (particularly in anatomically sensitive locations such as the femoral neck and the spine). Indeed, fractures in certain locations such as the femoral neck can prove to be fatal due to related complications such as DVT and PE.[66,67] Unfortunately, current imaging techniques are of limited value in quantifying bone metabolism and detecting aberrancies in the early stages of the disease before structural manifestation of decrease, such as decrease in bone mineral density. These early stages typically include (1) decreased rates of bone formation (deficiency in osteoblasts) and (2) excessive bone resorption (overactivity of osteoclasts). Conventional x-rays have been of limited

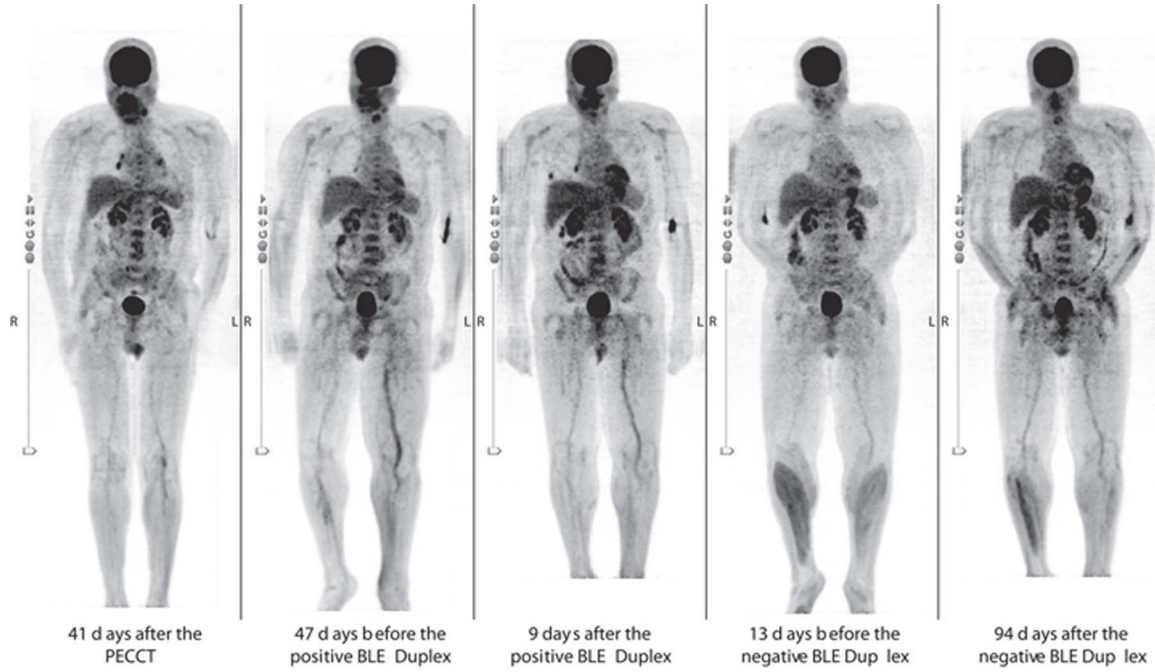

FIGURE 7. Chest computed tomography with pulmonary embolism protocol (PECCT) initially diagnosed patient 5 with PE at the right mainstem pulmonary artery 8 months before the bilateral lower extremities (BLE) Duplex diagnosed the patient with acute DVT at the left PV. A repeated BLE Duplex 2 months later was negative for acute DVT. From the left to the right are the FDG PETs 41 days after the PECCT and 47 days before and 9 days after the positive BLE Duplex, which demonstrate improvement from 47 days before with visualization of bilateral CF and PV only, and 13 days before and 94 days after the negative BLE Duplex for acute DVT, which demonstrate progression of visualization of bilateral CF, PV, left PT, and left peroneal. CF, common femoral; DVT, deep vein thrombosis; PECCT, chest CT with PE protocol; PT, posterior tibial; PV, popliteal vein; UE, upper extremity. Reproduced with permission from Zhu et al.[35]

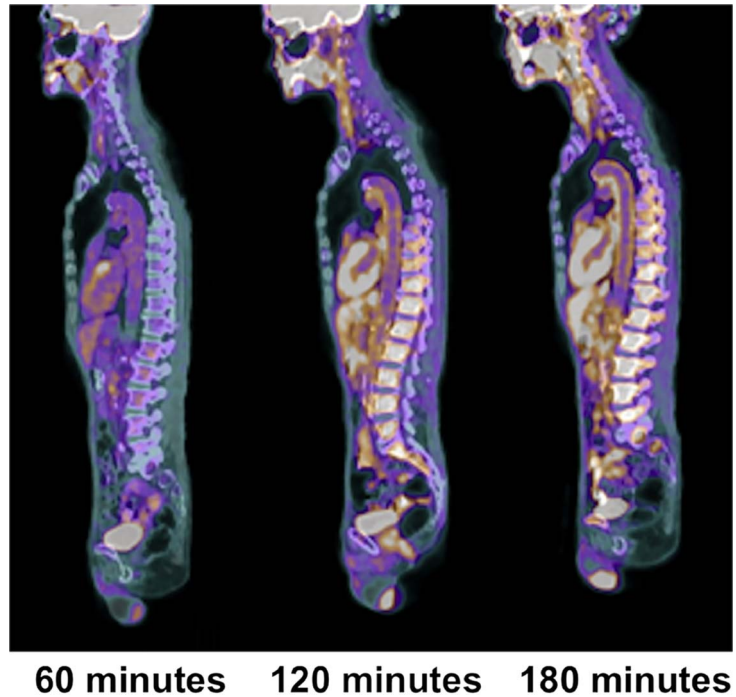

FIGURE 8. Changes in aortic wall and luminal blood FDG activity at different imaging time points as seen on sagittal FDG PET images of the thoracic aorta. With time, luminal blood activity decreases, whereas the aortic wall activity increases, which improves the arterial wall-to-blood contrast (superior target-to-background ratio). Reproduced with permission from Moghbel et al.[42]

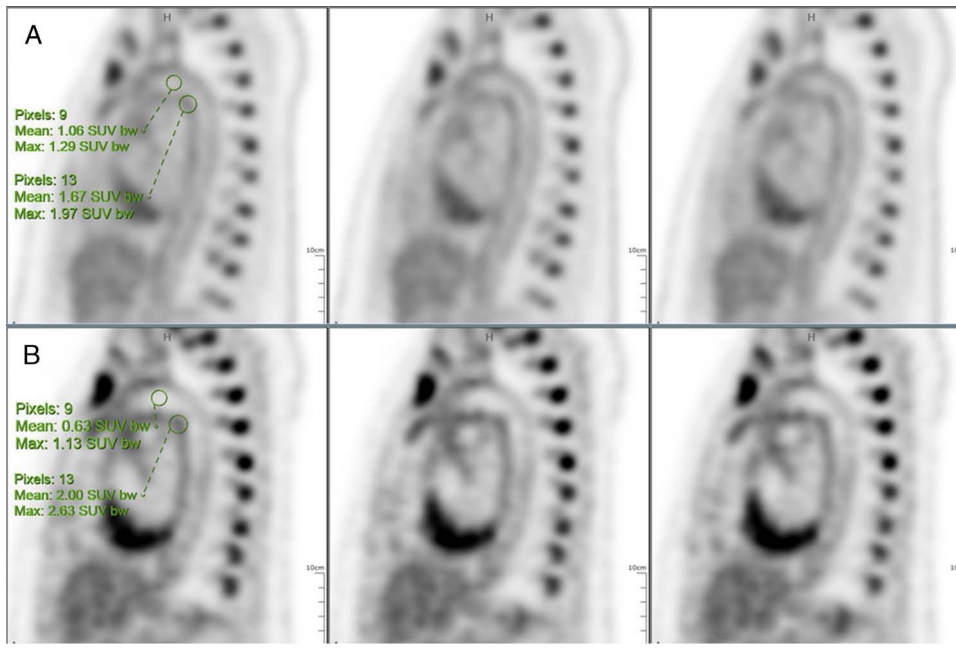

FIGURE 9. Delayed imaging provides more accurate diagnostic information. A 19-year-old girl with Takayasu arteritis underwent FDG PET/CT (dose 3.7 MBq/kg, acquisition time 15 minutes) to evaluate status of inflammation. PET images acquired 2 hours (**A**) and 5 hours (**B**) after FDG injection. The blood pool activity decreases (SUVmean 1.06–0.63), whereas the aortic wall FDG avidity increases (SUVmean from 1.61 to 2.00). The ratio between aortic wall and blood pool activities increases from 1.57 to 3.17. Reproduced with permission from Sui et al.[25]

value in detecting osteoporosis, particularly in the phases of the disease, as has been demonstrated by numerous studies over the past decades.[68,69] This has led to the adoption of dual-energy x-ray absorptiometry (DXA) as the modality of choice for detecting the disease and assessing the degree of response following various therapeutic interventions. However, an obvious issue with DXA in measuring bone mineral density is the fact that such scanners create bone density values by dividing the quotient of bone mineral content by total bone area. Naturally, this leads to larger bones appearing to be stronger but, in reality, possessing the same bone density as their smaller counterparts. Preliminary studies have attempted to correct for this by using overall bone size- and height-adjusted methodologies with mixed results.[70–72] Therefore, there is a dire need for an imaging modality that allows early detection and timely intervention of this very common metabolic bone disease without the shortfalls of DXA.

Sodium fluoride PET is a promising imaging tool to fill this need. Bone marrow uptake of this radiotracer is negligible, and NaF can freely diffuse to osteoblastic cells, allowing assessment of bone formation.[73] In past research, our laboratory and other investigators have used NaF PET to measure both age-related deterioration and osteoporotic degradation of a diverse range of bones such as the femoral neck and the spine (Fig. 12).[34,74–78] Because a reduction

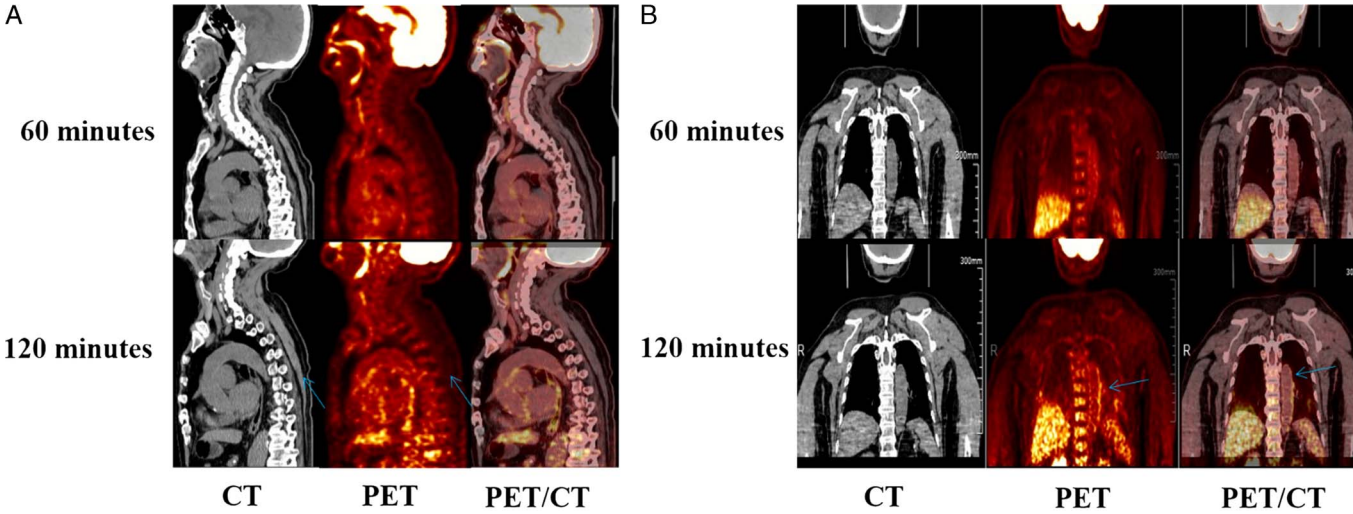

FIGURE 10. FDG PET/CT in a 84-year-old man with aortic AS. PET images 120 minutes delayed showed a significant increase in arterial wall metabolism compared with 60-minute PET images.

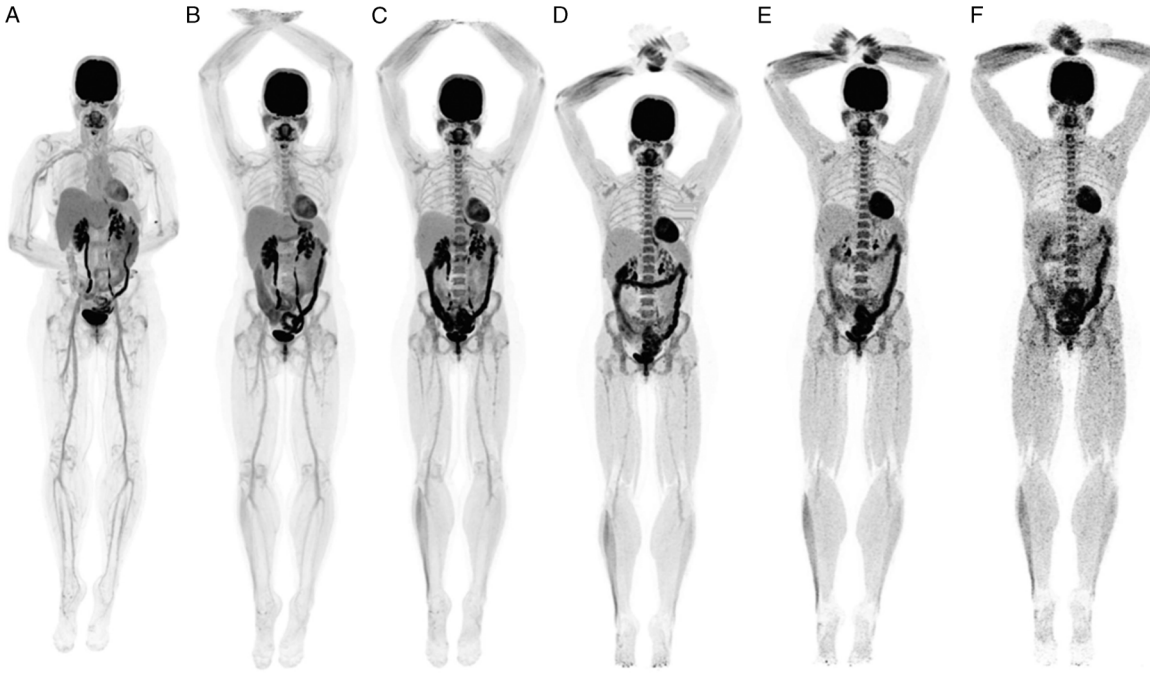

FIGURE 11. A 51-year-old female healthy volunteer. Dynamic scan was acquired for 60 minutes after injection of 348 MBq of FDG. **A**, Reconstruction of the last 20 minutes of dynamic acquisition; (**B**–**F**) 20-minute duration scans obtained at 90 minutes, and 3, 6, 9, and 12 hours after injection. Patient was fed with high-protein snack after the 3-hour scan. Reproduced with permission from PET Clinics.[61]

	MAV	SUVmax	SUVmean	pvcSUVmean	TCM	pvcTCM
Right Elbow	3.9	13.8	5.4	13.4	21.4	52.9
Left Elbow	7.5	10.7	5.5	15.8	40.8	118.0
Hands	18.8	39.3	13.6	28.8	254.4	540.3
TOTAL	30.2	63.8	24.5	58.0	316.6	711.2

	MAV	SUVmax	SUVmean	pvcSUVmean	TCM	pvcTCM
Right Knee	12.5	26.1	11.8	22.6	147	281.5
Left Knee	7.0	22.2	9.9	20.9	68.8	145.8
Right Foot	23.8	35.6	12.3	22.4	293.1	534.3
Left Foot	5.7	43.5	19.4	39.6	111.0	226.0
TOTAL	49.0	127.4	53.4	105.5	619.9	1187.6

FIGURE 12. NaF PET MIP of the upper body (**A**) and lower body (**B**) of an RA patient. Focal areas of high bone formation in the joints were segmented using an adaptive thresholding algorithm (ROVER software; ABX GmbH, Radeberg, Germany). Metabolically active volume (MAV), SUVmax, SUVmean, partial volume-corrected SUVmean (pvcSUVmean), total calcium metabolism (TCM), and partial volume-corrected TCM (pvcTCM) were calculated and summed for each segmented region. The global pvcTCM for this patient was 1898.8. Reproduced with permission from Saboury et al.[34]

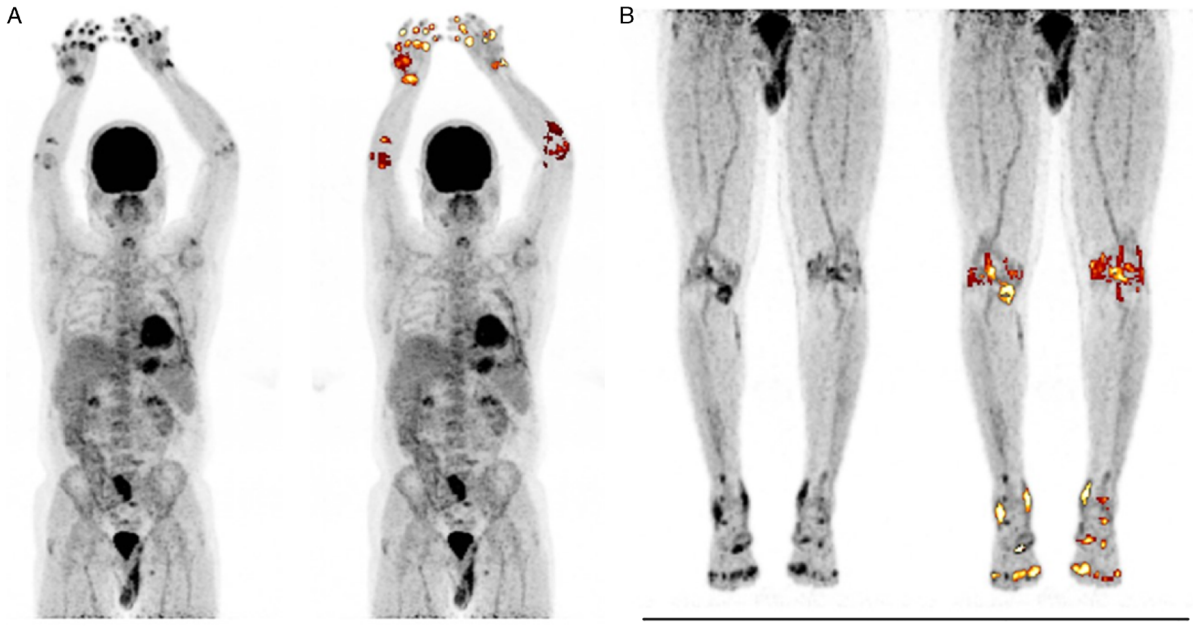

	MAV	SUVmax	SUVmean	pvcSUVmean	TLG	pvcTLG
Right Elbow	7.2	4.3	2.0	5.2	14.7	37.5
Left Elbow	20.0	3.4	1.5	3.7	29.9	74.1
Hands	41.8	8.8	3.3	7.0	136.3	292.4
TOTAL	69.0	16.5	6.8	15.9	180.9	404.0

	MAV	SUVmax	SUVmean	pvcSUVmean	TLG	pvcTLG
Right Knee	17.1	6.8	2.6	6.0	44.4	101.5
Left Knee	27.3	5.5	2.2	4.6	60.4	125.9
Right Foot	12.9	11.3	3.7	7.3	47.6	94.0
Left Foot	16.1	7.6	2.9	5.9	47.0	94.6
TOTAL	73.4	31.2	11.4	23.8	199.4	416.0

FIGURE 13. FDG PET MIP of the upper body (**A**) and lower body (**B**) of an RA patient. Synovial inflammation was assessed by segmenting FDG-avid joints using an adaptive thresholding algorithm (ROVER software; ABX GmbH, Radeberg, Germany). Metabolically active volume (MAV), SUVmax, SUVmean, partial volume-corrected SUVmean (pvcSUVmean), total lesion glycolysis (TLG), and partial volume-corrected TLG (pvcTLG) were calculated and summed for each segmented region. The global pvcTLG for this patient was 820.0. Reproduced with permission from Saboury et al.[34]

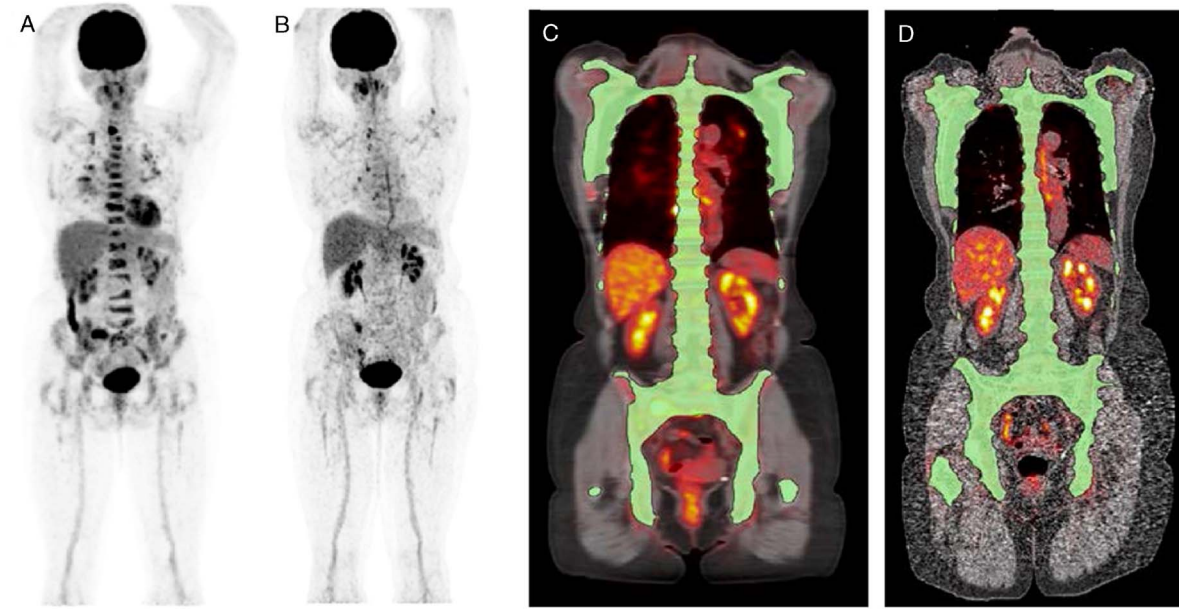

FIGURE 14. Potential role of global disease assessment by PET in multiple myeloma. FDG uptake changes of multiple myeloma lesions before (**A**) and after the treatment (**B**). High diffuse FDG uptake is observed in the entire spine before the treatment (**A**), whereas substantial reduction in FDG uptake is visually noted after the treatment (**B**). Segmentation of the entire skeleton followed by a closing algorithm allows for one to perform global disease assessment (OsiriX software; Pixmeo SARL, Bernex, Switzerland) (**C**, **D**). The pretreatment global average SUVmean (**C**) was 3.1 and decreased to 1.8 after the completion of the treatment (**D**). Reproduced with permission from Zadeh et al.[97]

in bone formation signals initial osteoporotic degradation, we can use NaF PET to detect the disease at the earliest time point when this disease can still be slowed by treatment with anabolic and/or antiresorptive agents. In addition, it can be used to assess response to therapy.

Besides the general factors such as increases in sensitivity and decreases in scanner time, TB-PET imaging offers several unique benefits when assessing degenerative bone disorders. First, TB-PET allows for the entire body to be scanned in a single acquisition. This is crucial for osteoporosis specifically, given that fragility fractures have been known to occur in the calcaneus.[79] In other words, this advancement from whole-body/region-specific to TB imaging will allow all possible osteoporotic bones to be assessed in a single acquisition instead of multiple series of scans. Another major benefit is being able to assess juvenile osteoporosis safely using TB NaF PET/CT. This is a rare disease of interest, given that there is little specific literature related to juvenile osteoporosis using NaF PET/CT to date, likely due to fears of excessive radiation exposure to children and adolescents.[80] However, with TB-PET instruments, there is a drastic decrease in radiation risk due to the substantial reduction in radiotracer dosage. Thus, TB imaging opens an entirely new avenue of applications for NaF PET imaging to assess metabolic bone diseases in the pediatric population.[81]

Systemic Inflammatory Disorders With Emphasis on MSK Abnormalities

Musculoskeletal disorders are major causes of disability in the general population with higher prevalence in the elderly subjects. The introduction of effective immunomodulatory treatments has substantially improved the outcome of these disorders in contrast to many other human maladies. Unfortunately, the role of clinical assessment, laboratory tests, and conventional imaging techniques is limited to either the diagnosis or monitoring the course of the disease, particularly following therapeutic interventions. Planar x-ray, CT, and MRI have been adopted as the modalities of choice for the diagnosis and routine follow-up of the affected populations.[82,83] Therefore, major decisions are made based on the results generated by these imaging modalities. As mentioned previously, the sensitivity and the specificity of structural imaging techniques are limited in any setting for diagnosing and following the course of many diseases and disorders. These deficiencies have led to overlooking the presence and the extent of many serious disorders and, sometimes, either overtreating or undertreating them during the course of the disease. Furthermore, many MSK abnormalities are systemic in nature and therefore affect many organs and anatomic structures throughout the body during the course of the disease. Therefore, there is a need for a modality that allows systemic and TB assessment about the presence, the extent, and the degree of disease activity throughout the body with one single data acquisition. Many rheumatologic diseases including rheumatoid arthritis (RA), vasculitis, and myositis are systemic in nature, and therefore, their management will significantly benefit from TB-PET imaging.[84–89] For example, RA not only affects the joints throughout the body, but it has also been shown commonly to be associated with high incidence of AS and shorter life span. Similarly, many autoimmune disorders suffer from structural and functional muscle disease, which further affects the subject's ability to perform daily routine activities. Therefore, TB-PET imaging will allow disease assessment of the joints, muscles, and other organ systems, and this will improve the management of patients with these common autoimmune disorders. In particular, detection of AS by either FDG or NaF PET imaging may play a major role in preventing early death due to RA in the early stages of the disease (Fig. 13).[34]

Importance of Global Disease Assessment Score and System-Biology Imaging

Over the past 3 decades, we have been emphasizing the importance of global disease assessment of the involved organs by systemic diseases and disorders.[41,90–95] We believe that regional assessment of such abnormalities alone will be of limited value in the overall diagnosis and management of such serious human maladies.[96] With the advances that have been made in optimal quantification of the global disease activity in various organs and throughout the body, the potential role of TB imaging has been enhanced and clearly realized (Fig. 14).[97] We have to emphasize the importance of certain issues that relate to accurate PET quantification at the regional level including partial volume correction of the tracer uptake in various organ sites. Accurate calculation of regional activity at the disease sites will allow measuring TB disease burden with this approach. Underestimation of regional and global values that are related to respiratory and cardiac motions needs to be taken into consideration for such measurements. Again, the unavoidable effects of such physiological movements are somewhat minimal with the TB-PET instruments than with the conventional machines. In addition, interaction of various biological systems throughout the process of pathogenesis could be investigated using these techniques. The essential role of immune system, beyond infectious host defense, in the process of oncogenesis or atherogenesis is a well-established phenomenon.[98] Quantification of each system's function using global disease assessment paradigm and then investigation of their network of relations (synchronous and metachronous temporospatial models) is system biology par excellence in clinical medicine.[99] PET imaging with novel quantitative techniques introduced in recent years will provide physicians with a single number that represents the entire body disease burden, which may be used to test and validate the efficacy of novel interventions.

REFERENCES

1. Hounsfield GN. Computerized transverse axial scanning (tomography). 1. Description of system. *Br J Radiol*. 1973;46:1016–1022.
2. Lauterbur PC. Image formation by induced local interactions: examples employing nuclear magnetic resonance. *Nature*. 1973;242:190–191.
3. Mansfield P, Maudsley AA. Medical imaging by NMR. *Br J Radiol*. 1977;50:188–194.
4. Kuhl DE, Edwards RQ. Image separation radioisotope scanning. *Radiology*. 1963;80:653–662.
5. Budinger TF, Rollo FD. Physics and instrumentation. *Prog Cardiovasc Dis*. 1977;20:19–53.
6. Keyes JW Jr., Orlandea N, Heetderks WJ, et al. The Humongotron—a scintillation-camera transaxial tomograph. *J Nucl Med*. 1977;18:381–387.
7. Alavi A, Basu S. Planar and SPECT imaging in the era of PET and PET-CT: can it survive the test of time? *Eur J Nucl Med Mol Imaging*. 2008;35:1554–1559.
8. Ter-Pogossian MM, Phelps ME, Hoffman EJ, et al. A positron-emission transaxial tomograph for nuclear imaging (PETT). *Radiology*. 1975;114:89–98.
9. Alavi A, Reivich M. Guest editorial: the conception of FDG-PET imaging. *Semin Nucl Med*. 2002;32:2–5.
10. Ido T, Wan CN, Casella V, et al. Labeled 2-deoxy-D-glucose analogs. ^{18}F-labeled 2-deoxy-2-fluoro-D-glucose, 2-deoxy-2-fluoro-D-mannose and ^{14}C-2-deoxy-2-fluoro-D-glucose. *J Label Comp Radiopharm*. 1978;14:175–183.
11. Alessio AM, Kinahan PE, Cheng PM, et al. PET/CT scanner instrumentation, challenges, and solutions. *Radiol Clin North Am*. 2004;42:1017–1032, vii.
12. Badawi RD, Shi H, Hu P, et al. First human imaging studies with the EXPLORER total-body PET scanner. *J Nucl Med*. 2019;60:299–303.
13. Hustinx R, Bénard F, Alavi A. Whole-body FDG-PET imaging in the management of patients with cancer. *Semin Nucl Med*. 2002;32:35–46.
14. Gambhir SS. Molecular imaging of cancer with positron emission tomography. *Nat Rev Cancer*. 2002;2:683–693.
15. Pauwels EKJ, Ribeiro MJ, Stoot JHMB, et al. FDG accumulation and tumor biology. *Nucl Med Biol*. 1998;25:317–322.

16. Zhuang H, Pourdehnad M, Lambright ES, et al. Dual time point ^{18}F-FDG PET imaging for differentiating malignant from inflammatory processes. *J Nucl Med*. 2001;42:1412–1417.
17. Basu S, Kung J, Houseni M, et al. Temporal profile of fluorodeoxyglucose uptake in malignant lesions and normal organs over extended time periods in patients with lung carcinoma: implications for its utilization in assessing malignant lesions. *Q J Nucl Med Mol Imaging*. 2009;53:9–19.
18. Cheng G, Alavi A, Lim E, et al. Dynamic changes of FDG uptake and clearance in normal tissues. *Mol Imaging Biol*. 2013;15:345–352.
19. Cherry SR, Jones T, Karp JS, et al. Total-body PET: maximizing sensitivity to create new opportunities for clinical research and patient care. *J Nucl Med*. 2018;59:3–12.
20. Zhang X, Cherry SR, Xie Z, et al. Subsecond total-body imaging using ultrasensitive positron emission tomography. *Proc Natl Acad Sci U S A*. 2020; 117:2265–2267.
21. Spencer BA, Berg E, Schmall JP, et al. Performance evaluation of the uEXPLORER total-body PET/CT scanner based on NEMA NU 2-2018 with additional tests to characterize PET scanners with a long axial field of view. *J Nucl Med*. 2021;62:861–870.
22. Hustinx R, Smith RJ, Benard F, et al. Dual time point fluorine-18 fluorodeoxyglucose positron emission tomography: a potential method to differentiate malignancy from inflammation and normal tissue in the head and neck. *Eur J Nucl Med*. 1999;26:1345–1348.
23. Kumar R, Loving VA, Chauhan A, et al. Potential of dual-time-point imaging to improve breast cancer diagnosis with (18)F-FDG PET. *J Nucl Med*. 2005; 46:1819–1824.
24. Basu S, Torigian D, Alavi A. Evolving concept of imaging bone marrow metastasis in the twenty-first century: critical role of FDG-PET. *Eur J Nucl Med Mol Imaging*. 2008;35:465–471.
25. Sui X, Liu G, Hu P, et al. Total-body PET/computed tomography highlights in clinical practice: experiences from Zhongshan Hospital, Fudan University. *PET Clin*. 2021;16:9–14.
26. Nardo L, Pantel AR. Oncologic applications of long axial field-of-view PET/computed tomography. *PET Clin*. 2021;16:65–73.
27. Yun M, Yeh D, Araujo LI, et al. F-18 FDG uptake in the large arteries: a new observation. *Clin Nucl Med*. 2001;26:314–319.
28. Sydow BD, Srinivas SM, Newberg A, et al. Deep venous thrombosis on F-18 FDG PET/CT imaging. *Clin Nucl Med*. 2006;31:403–404.
29. Sharma P, Kumar R, Singh H, et al. Imaging thrombus in cancer patients with FDG PET-CT. *Jpn J Radiol*. 2012;30:95–104.
30. Hess S, Madsen PH, Basu S, et al. Potential role of FDG PET/CT imaging for assessing venous thromboembolic disorders. *Clin Nucl Med*. 2012;37: 1170–1172.
31. Chang KJ, Zhuang H, Alavi A. Detection of chronic recurrent lower extremity deep venous thrombosis on fluorine-18 fluorodeoxyglucose positron emission tomography. *Clin Nucl Med*. 2000;25:838–839.
32. Houshmand S, Salavati A, Hess S, et al. Detection of deep vein thrombosis using FDG-PET/CT volumetric parameters: a diagnostic performance study. *Soc Nuclear Med*. 2015.
33. Saha P, Humphries J, Modarai B, et al. Leukocytes and the natural history of deep vein thrombosis: current concepts and future directions. *Arterioscler Thromb Vasc Biol*. 2011;31:506–512.
34. Saboury B, Morris MA, Nikpanah M, et al. Reinventing molecular imaging with total-body PET, part II: clinical applications. *PET Clin*. 2020;15: 463–475.
35. Zhu HJ, Hess S, Rubello D, et al. The strong but nonspecific relationship between ^{18}F-FDG uptake in the lower-extremity veins and venous thromboembolism. *Nucl Med Commun*. 2016;37:322–328.
36. Ross JS, Stagliano NE, Donovan MJ, et al. Atherosclerosis and cancer: common molecular pathways of disease development and progression. *Ann N Y Acad Sci*. 2001;947:271–292; discussion 273–292.
37. Ross JS, Stagliano NE, Donovan MJ, et al. Atherosclerosis: a cancer of the blood vessels? *Am J Clin Pathol*. 2001;116(suppl):S97–S107.
38. Tapia-Vieyra JV, Delgado-Coello B, Mas-Oliva J. Atherosclerosis and cancer; a resemblance with far-reaching implications. *Arch Med Res*. 2017;48: 12–26.
39. Ogawa A, Kanda T, Sugihara S, et al. Risk factors for myocardial infarction in cancer patients. *J Med*. 1995;26:221–233.
40. Dardiotis E, Aloizou A-M, Markoula S, et al. Cancer-associated stroke: pathophysiology, detection and management [review]. *Int J Oncol*. 2019;54: 779–796.
41. Beheshti M, Saboury B, Mehta NN, et al. Detection and global quantification of cardiovascular molecular calcification by fluoro18-fluoride positron emission tomography/computed tomography—a novel concept. *Hell J Nucl Med*. 2011;14:114–120.
42. Moghbel M, Al-Zaghal A, Werner TJ, et al. The role of PET in evaluating atherosclerosis: a critical review. *Semin Nucl Med*. 2018;48:488–497.
43. Høilund-Carlsen PF, Sturek M, Alavi A, et al. Atherosclerosis imaging with (18)F-sodium fluoride PET: state-of-the-art review. *Eur J Nucl Med Mol Imaging*. 2020;47:1538–1551.
44. Schmall JP, Karp JS, Alavi A. The potential role of total body PET imaging in assessment of atherosclerosis. *PET Clin*. 2019;14:245–250.
45. Herrington W, Lacey B, Sherliker P, et al. Epidemiology of atherosclerosis and the potential to reduce the global burden of atherothrombotic disease. *Circ Res*. 2016;118:535–546.
46. World Health Organization. Available at: https://www.who.int/data/gho/data/themes/mortality-and-global-health-estimates. Accessed October 16, 2021.
47. Benjamin EJ, Muntner P, Alonso A, et al. Heart disease and stroke statistics—2019 update: a report from the American Heart Association. *Circulation*. 2019;139:e56–e528.
48. Wilms G, Baert AL. The history of angiography. *J Belge Radiol*. 1995;78: 299–302.
49. Agatston AS, Janowitz WR, Hildner FJ, et al. Quantification of coronary artery calcium using ultrafast computed tomography. *J Am Coll Cardiol*. 1990; 15:827–832.
50. Willemink MJ, van der Werf NR, Nieman K, et al. Coronary artery calcium: a technical argument for a new scoring method. *J Cardiovasc Comput Tomogr*. 2019;13:347–352.
51. Alavi A, Werner TJ, Høilund-Carlsen PF. PET-based imaging to detect and characterize cardiovascular disorders: unavoidable path for the foreseeable future. *J Nucl Cardiol*. 2018;25:203–207.
52. Alavi A, Werner TJ, Høilund-Carlsen PF. What can be and what cannot be accomplished with PET to detect and characterize atherosclerotic plaques. *J Nucl Cardiol*. 2018;25:2012–2015.
53. Narula J, Kovacic JC. Putting TCFA in clinical perspective. *J Am Coll Cardiol*. 2014;64:681–683.
54. Arbab-Zadeh A, Fuster V. The myth of the "vulnerable plaque": transitioning from a focus on individual lesions to atherosclerotic disease burden for coronary artery disease risk assessment. *J Am Coll Cardiol*. 2015;65:846–855.
55. Blomberg BA, de Jong PA, Thomassen A, et al. Thoracic aorta calcification but not inflammation is associated with increased cardiovascular disease risk: results of the CAMONA study. *Eur J Nucl Med Mol Imaging*. 2017; 44:249–258.
56. McKenney-Drake ML, Moghbel MC, Paydary K, et al. ^{18}F-NaF and ^{18}F-FDG as molecular probes in the evaluation of atherosclerosis. *Eur J Nucl Med Mol Imaging*. 2018;45:2190–2200.
57. Fiz F, Morbelli S, Bauckneht M, et al. Correlation between thoracic aorta ^{18}F-natrium fluoride uptake and cardiovascular risk. *World J Radiol*. 2016; 8:82–89.
58. Blomberg BA, Thomassen A, Takx RAP, et al. Delayed ^{18}F-fluorodeoxyglucose PET/CT imaging improves quantitation of atherosclerotic plaque inflammation: results from the CAMONA study. *J Nucl Cardiol*. 2014;21:588–597.
59. Blomberg BA, Thomassen A, Takx RAP, et al. Delayed sodium ^{18}F-fluoride PET/CT imaging does not improve quantification of vascular calcification metabolism: results from the CAMONA study. *J Nucl Cardiol*. 2014;21:293–304.
60. Kwiecinski J, Berman DS, Lee SE, et al. Three-hour delayed imaging improves assessment of coronary ^{18}F-sodium fluoride PET. *J Nucl Med*. 2019;60:530–535.
61. Nardo L, Abdelhafez YG, Spencer BA, et al. Clinical implementation of total-body PET/CT at University of California, Davis. *PET Clin*. 2021;16:1–7.
62. Bäck M, Hansson GK. Anti-inflammatory therapies for atherosclerosis. *Nat Rev Cardiol*. 2015;12:199–211.
63. Solanki A, Bhatt LK, Johnston TP. Evolving targets for the treatment of atherosclerosis. *Pharmacol Ther*. 2018;187:1–12.
64. Ji M-X, Yu Q. Primary osteoporosis in postmenopausal women. *Chron Dis Transl Med*. 2015;1:9–13.
65. Eastell R, O'Neill TW, Hofbauer LC, et al. Postmenopausal osteoporosis. *Nat Rev Dis Primers*. 2016;2:16069.
66. Hitos K, Fletcher JP. Venous thromboembolism and fractured neck of femur. *Thromb Haemost*. 2005;94:991–996.
67. Fu YH, Liu P, Xu X, et al. Deep vein thrombosis in the lower extremities after femoral neck fracture: a retrospective observational study. *J Orthop Surg (Hong Kong)*. 2020;28:2309499019901172.
68. Brunader R, Shelton DK. Radiologic bone assessment in the evaluation of osteoporosis. *Am Fam Physician*. 2002;65:1357–1364.

69. Guglielmi G, Muscarella S, Bazzocchi A. Integrated imaging approach to osteoporosis: state-of-the-art review and update. *Radiographics*. 2011;31:1343–1364.
70. Zemel BS, Leonard MB, Kelly A, et al. Height adjustment in assessing dual energy x-ray absorptiometry measurements of bone mass and density in children. *J Clin Endocrinol Metab*. 2010;95:1265–1273.
71. Crabtree NJ, Högler W, Cooper MS, et al. Diagnostic evaluation of bone densitometric size adjustment techniques in children with and without low trauma fractures. *Osteoporos Int*. 2013;24:2015–2024.
72. Choksi P, Jepsen KJ, Clines GA. The challenges of diagnosing osteoporosis and the limitations of currently available tools. *Clin Diabetes Endocrinol*. 2018;4:12–12.
73. Raynor W, Houshmand S, Gholami S, et al. Evolving role of molecular imaging with (18)F-sodium fluoride PET as a biomarker for calcium metabolism. *Curr Osteoporos Rep*. 2016;14:115–125.
74. Uchida K, Nakajima H, Miyazaki T, et al. Effects of alendronate on bone metabolism in glucocorticoid-induced osteoporosis measured by ^{18}F-fluoride PET: a prospective study. *J Nucl Med*. 2009;50:1808–1814.
75. Raynor W, Houshmand S, Gholami S, et al. Assessment of bone turnover by measuring global uptake of ^{18}F-sodium fluoride in the femoral neck, a novel method for early detection of osteoporosis. *J Nucl Med*. 2016;57:1769–1769.
76. McHugh C, Raynor W, Werner T, et al. Quantification of bone metabolism in the hip and spine using PET/MRI/CT. *J Nucl Med*. 2017;58:1225–1225.
77. Ayubcha C, Zirakchian Zadeh M, Stochkendahl MJ, et al. Quantitative evaluation of normal spinal osseous metabolism with ^{18}F-NaF PET/CT. *Nucl Med Commun*. 2018;39:945–950.
78. Rhodes S, Batzdorf A, Sorci O, et al. Assessment of femoral neck bone metabolism using ^{18}F-sodium fluoride PET/CT imaging. *Bone*. 2020;136:115351.
79. Ito K, Hori K, Terashima Y, et al. Insufficiency fracture of the body of the calcaneus in elderly patients with osteoporosis: a report of two cases. *Clin Orthop Relat Res*. 2004;422:190–194.
80. Fahey FH. Dosimetry of pediatric PET/CT. *J Nucl Med*. 2009;50:1483–1491.
81. Nardo L, Schmall JP, Werner TJ, et al. Potential roles of total-body PET/computed tomography in pediatric imaging. *PET Clin*. 2020;15:271–279.
82. Korb-Pap A, Stratis A, Mühlenberg K, et al. Early structural changes in cartilage and bone are required for the attachment and invasion of inflamed synovial tissue during destructive inflammatory arthritis. *Ann Rheum Dis*. 2012;71:1004–1011.
83. Palmer AJ, Brown CP, McNally EG, et al. Non-invasive imaging of cartilage in early osteoarthritis. *Bone Joint J*. 2013;95-B:738–746.
84. Dhawan R, Lokitz K, Lokitz S, et al. FDG PET imaging of extremities in rheumatoid arthritis. *J La State Med Soc*. 2016;168:156–161.
85. Hirata Y, Inaba Y, Kobayashi N, et al. Correlation between mechanical stress by finite element analysis and ^{18}F-fluoride PET uptake in hip osteoarthritis patients. *J Orthop Res*. 2015;33:78–83.
86. Kobayashi N, Inaba Y, Tateishi U, et al. New application of ^{18}F-fluoride PET for the detection of bone remodeling in early-stage osteoarthritis of the hip. *Clin Nucl Med*. 2013;38:e379–e383.
87. Kobayashi N, Inaba Y, Tateishi U, et al. Comparison of ^{18}F-fluoride positron emission tomography and magnetic resonance imaging in evaluating early-stage osteoarthritis of the hip. *Nucl Med Commun*. 2015;36:84–89.
88. Kothekar E, Borja AJ, Gerke O, et al. Assessing respitatory muscle activity with ^{18}F-FDG-PET/CT in patients with COPD. *Am J Nucl Med Mol Imaging*. 2019;9:309–315.
89. Kothekar E, Yellanki D, Borja AJ, et al. ^{18}F-FDG-PET/CT in measuring volume and global metabolic activity of thigh muscles: a novel CT-based tissue segmentation methodology. *Nucl Med Commun*. 2020;41:162–168.
90. Alavi A, Newberg AB, Souder E, et al. Quantitative analysis of PET and MRI data in normal aging and Alzheimer's disease: atrophy weighted total brain metabolism and absolute whole brain metabolism as reliable discriminators. *J Nucl Med*. 1993;34:1681–1687.
91. Bural GG, Torigian DA, Chamroonrat W, et al. Quantitative assessment of the atherosclerotic burden of the aorta by combined FDG-PET and CT image analysis: a new concept. *Nucl Med Biol*. 2006;33:1037–1043.
92. Berkowitz A, Basu S, Srinivas S, et al. Determination of whole-body metabolic burden as a quantitative measure of disease activity in lymphoma: a novel approach with fluorodeoxyglucose-PET. *Nucl Med Commun*. 2008;29:521–526.
93. Basu S, Saboury B, Werner T, et al. Clinical utility of FDG-PET and PET/CT in non-malignant thoracic disorders. *Mol Imaging Biol*. 2011;13:1051–1060.
94. Abdulla S, Salavati A, Saboury B, et al. Quantitative assessment of global lung inflammation following radiation therapy using FDG PET/CT: a pilot study. *Eur J Nucl Med Mol Imaging*. 2014;41:350–356.
95. Saboury B, Salavati A, Brothers A, et al. FDG PET/CT in Crohn's disease: correlation of quantitative FDG PET/CT parameters with clinical and endoscopic surrogate markers of disease activity. *Eur J Nucl Med Mol Imaging*. 2014;41:605–614.
96. Høilund-Carlsen PF, Edenbrandt L, Alavi A. Global Disease Score (GDS) is the name of the game! *Eur J Nucl Med Mol Imaging*. 2019;46:1768–1772.
97. Zadeh MZ, Raynor WY, Seraj SM, et al. Evolving roles of fluorodeoxyglucose and sodium fluoride in assessment of multiple myeloma patients: introducing a novel method of PET quantification to overcome shortcomings of the existing approaches. *PET Clin*. 2019;14:341–352.
98. Rankin LC, Artis D. Beyond host defense: emerging functions of the immune system in regulating complex tissue physiology. *Cell*. 2018;173:554–567.
99. Pinu FR, Beale DJ, Paten AM, et al. Systems biology and multi-omics integration: viewpoints from the metabolomics research community. *Metabolites*. 2019;9.